

## Central Lancashire Online Knowledge (CLoK)

Title	EPIC 201585823, a rare triple-mode RR Lyrae star discovered in K2 mission data
Type	Article
URL	<a href="https://clock.uclan.ac.uk/id/eprint/14602/">https://clock.uclan.ac.uk/id/eprint/14602/</a>
DOI	<a href="https://doi.org/10.1093/mnras/stv2377">https://doi.org/10.1093/mnras/stv2377</a>
Date	2016
Citation	Kurtz, Donald Wayne, Bowman, D. M., Ebo, S. J., Moskalik, P., Handberg, R. and Lund, M. N. (2016) EPIC 201585823, a rare triple-mode RR Lyrae star discovered in K2 mission data. Monthly Notices of the Royal Astronomical Society, 455 (2). pp. 1237-1245. ISSN 0035-8711
Creators	Kurtz, Donald Wayne, Bowman, D. M., Ebo, S. J., Moskalik, P., Handberg, R. and Lund, M. N.

It is advisable to refer to the publisher's version if you intend to cite from the work.  
<https://doi.org/10.1093/mnras/stv2377>

For information about Research at UCLan please go to <http://www.uclan.ac.uk/research/>

All outputs in CLoK are protected by Intellectual Property Rights law, including Copyright law. Copyright, IPR and Moral Rights for the works on this site are retained by the individual authors and/or other copyright owners. Terms and conditions for use of this material are defined in the <http://clock.uclan.ac.uk/policies/>

# EPIC 201585823, a rare triple-mode RR Lyrae star discovered in K2 mission data

Donald W. Kurtz,<sup>1★</sup> Dominic M. Bowman,<sup>1</sup> Simon J. Ebo,<sup>1</sup> Paweł Moskalik,<sup>2</sup> Rasmus Handberg<sup>3</sup> and Mikkel N. Lund<sup>3</sup>

<sup>1</sup>Jeremiah Horrocks Institute, University of Central Lancashire, Preston PR1 2HE, UK

<sup>2</sup>Copernicus Astronomical Center, ul. Bartycka 18, PL-00-716 Warsaw, Poland

<sup>3</sup>Stellar Astrophysics Centre (SAC), Department of Physics and Astronomy, Aarhus University, Ny Munkegade 120, DK-8000 Aarhus C, Denmark

Accepted 2015 October 11. Received 2015 October 5; in original form 2015 August 5

## ABSTRACT

We have discovered a new, rare triple-mode RR Lyr star, EPIC 201585823, in the *Kepler* K2 mission Campaign 1 data. This star pulsates primarily in the fundamental and first-overtone radial modes, and, in addition, a third non-radial mode. The ratio of the period of the non-radial mode to that of the first-overtone radial mode, 0.616 285, is remarkably similar to that seen in 11 other triple-mode RR Lyr stars, and in 260 RRC stars observed in the Galactic bulge. This systematic character promises new constraints on RR Lyr star models. We detected subharmonics of the non-radial mode frequency, which are a signature of period doubling of this oscillation; we note that this phenomenon is ubiquitous in RRC and RRd stars observed from space, and from ground with sufficient precision. The non-radial mode and subharmonic frequencies are not constant in frequency or in amplitude. The amplitude spectrum of EPIC 201585823 is dominated by many combination frequencies among the three interacting pulsation mode frequencies. Inspection of the phase relationships of the combination frequencies in a phasor plot explains the ‘upward’ shape of the light curve. We also found that raw data with custom masks encompassing all pixels with significant signal for the star, but without correction for pointing changes, is best for frequency analysis of this star, and, by implication, other RR Lyr stars observed by the K2 mission. We compare several pipeline reductions of the K2 mission data for this star.

**Key words:** asteroseismology – stars: individual: EPIC 201585823 – stars: oscillations – stars: variables: RR Lyrae.

## 1 INTRODUCTION

RR Lyrae stars were first noted in the 1890s by Solon Bailey, Wilhelmina Fleming and Edward Pickering. At first, they were known as cluster variables because so many were found in globular clusters. Those variables, along with globular cluster Cepheids, allowed Harlow Shapley, in his ‘Studies of Magnitudes in Star Clusters’ series of papers beginning in 1916, to measure distances to the globular clusters and show that the Sun lies far from the centre of the Milky Way, using Henrietta Leavitt’s now-famous 1912 period–luminosity relation (Leavitt & Pickering 1912), along with Ejnar Hertzsprung’s 1913 calibration using statistical parallaxes of 13 Cepheids (Hertzsprung 1913). In the early decades of the 20th century the RR Lyr stars had made their mark as distance indicators, and it is that for which they are still best known.

Solon Bailey first classified the light curves of RR Lyr stars phenomenologically into three sub-classes, ‘a’, ‘b’ and ‘c’, in his

252 page magnum opus on over 500 variable stars in  $\omega$  Cen (Bailey 1902). Bailey’s classes ‘a’ and ‘b’ stars are now consolidated into a class known as RRab stars that pulsate in the fundamental radial mode and have strongly non-sinusoidal light curves; his class ‘c’ stars are now known as RRC stars, which are variables that pulsate in the first-overtone radial mode with more sinusoidal variations.

Edward Pickering, the director of the Harvard College Observatory, noted in the preface to Bailey’s work: ‘Nearly all of these stars appear to vary with perfect regularity so that the period can be determined, in some cases, within a fraction of a second’. Yet it was a mere five years later that Blažko (1907) first noted modulation of the light curve of the RR Lyr star RW Dra. He reported that the period varied between  $10^h35^m36^s$  and  $10^h40^m02^s$  in the time span of 41.6 d. So much for Pickering’s ‘perfect’ regularity! Modulation in RR Lyr light curves is common and now known as the Blažhko effect, a term first used by Tsevevich (1953). (‘Blažhko’ is now the spelling universally used, rather than the original spelling of ‘Blažko’.) This effect is not yet fully understood.

Jerzykiewicz & Wenzel (1977) discovered that AQ Leo is an RR Lyr star pulsating in two modes that are non-linearly

\* E-mail: dwkurtz@uclan.ac.uk

interacting, generating many combination frequencies. That was the first ‘double mode’ RR Lyr star discovered, hence can be considered to be the prototype of the class. Since then, nearly 2000 more such stars have been found (Moskalik 2014), and they are now known as RRd stars. The ‘d’ in RRd fits nicely in sequence with Bailey’s ‘a’, ‘b’ and ‘c’, and fortuitously it also can be construed to mean ‘d’ for double mode. Typically, the double mode RR Lyr stars pulsate in the fundamental and first-overtone radial modes with a period ratio close to 0.74 for most such stars and usually the first-overtone mode has the higher amplitude (Moskalik 2013).

More recently, other RRc stars have been found pulsating in two modes, the first-overtone radial mode and a non-radial mode with frequency between the third and fourth overtone radial modes with a period ratio with respect to the dominant first-overtone radial mode near to 0.61 (the range is 0.595–0.634). While these stars are relatively rare compared to all known RR Lyr stars, many are now known. The first RRc stars with the 0.61 period ratio were found by Olech & Moskalik (2009), who found two unambiguous cases in  $\omega$  Cen, V19 and V105, which they announced to be the first members of a new class of double mode RR Lyr stars. A few years later Moskalik et al. (2015) listed only 19 such stars (their table 8); Jursik et al. (2015) added 14 more (their table 3) in a new study of RR Lyr stars in M3 (which is one of the first globular clusters studied for RR Lyr stars in the first decade of the 1900s by the Harvard group).

The number has now exploded dramatically with 145 such RRc stars discovered by Netzel, Smolec & Moskalik (2015a) in the Galactic bulge using OGLE-III data,<sup>1</sup> although this represents only 3 per cent of the sample in that study. In another study of Galactic bulge RR Lyr stars using OGLE-IV data<sup>1</sup>, Netzel, Smolec & Moskalik (2015b) analysed 485 RRc stars. They found non-radial modes with the period ratio near 0.61 in 131 RRc stars (115 of which are new discoveries). The occurrence rate is 27 per cent. The OGLE-IV data have a much higher data density than the OGLE-III data, which results in lower noise in the amplitude spectra; thus, as expected, there is a higher occurrence rate in the OGLE-IV data. Combining results of OGLE-IV and OGLE-III, there are now 260 RRc stars known in the Galactic bulge with the non-radial mode with the 0.61 period ratio.

While RRc stars pulsating in the radial first-overtone mode and a non-radial mode with period ratio near to 0.61 are no longer rare, triple-mode RR Lyr stars are still rare. Gruberbauer et al. (2007) observed the prototype RRd star, AQ Leo, with the *MOST* satellite for 34.4 d and found, in addition to a large number of non-linear combination frequencies, evidence for other, non-combination frequencies that they conjectured may be associated with additional modes. We can now see that they found a non-radial mode with the 0.61 period ratio with respect to the first-overtone radial mode. Chadid (2012) then found triple-mode pulsation in the RRd star CoRoT 101368812, where the dominant mode frequencies have a ratio of 0.745, typical of fundamental and first-overtone radial modes in RRd stars, plus a third frequency belonging to a non-radial mode with a period ratio of 0.61 with respect to the first-overtone radial mode frequency. Two more such stars were found in K2 data

by Molnár et al. (2015); three were found in the Galactic bulge by Netzel et al. (2015a) and Smolec et al. (2015a); and four were found in M3 by Jursik et al. (2015). Those 11, plus our discovery of triple-mode pulsation in EPIC 201585823, brings to 12 the known triple-mode RR Lyr stars with the 0.61 period ratio. We list them with references in Section 2.4.

Yet another triple-mode RR Lyr variable was discovered by Smolec et al. (2015b) in the OGLE-IV photometry of the Galactic bulge. This star, OGLE-BLG-RRLYR-24137, pulsates in the radial fundamental mode, the radial first-overtone mode and a third mode with a period ratio of 0.686 to the radial first overtone. This period ratio is very different from the 0.61 ratio observed in the RR Lyr stars discussed above. Thus, OGLE-BLG-RRLYR-24137 is a (currently) unique object, not similar to any other known RR Lyr pulsator. It will, therefore, not be discussed further in this paper.

Moskalik & Buchler (1990) showed theoretically that any half-integer resonance (e.g. 3:2, 5:2, etc.) between two pulsation modes can cause ‘period doubling’, a characteristic alternating of the amplitudes of the maxima or minima in the light curve. These alternations are represented in the Fourier spectrum by subharmonics, that is by peaks at  $(n + \frac{1}{2})f$ , where  $n$  is integer and  $f$  is the frequency of the period-doubled mode. Pulsations with such characteristics have been known for decades in the RV Tauri variables (for a review see e.g. Wallerstein 2002). They were also predicted by Buchler & Moskalik (1992), then discovered by Smolec et al. (2012) in at least one BL Herculis star, BLG184.7 133264 (BL Her stars are a short period subgroup of the Population II Cepheids).

In the RR Lyrae stars, period doubling was first found (somewhat unexpectedly) by Szabó et al. (2010), who detected it in RR Lyr itself and in two other RRab variables observed by the *Kepler* space telescope. From hydrodynamic models, Kolláth, Molnár & Szabó (2011) then traced the period doubling in those stars to a 9:2 resonance between the ninth radial overtone and the fundamental radial mode. Moskalik et al. (2015) found period doubling of the non-radial 0.61 period ratio modes in four RRc stars observed by *Kepler*. They also noted from the literature a similar period doubling in two other RRc stars and four RRd stars observed from space (see their table 8), showing that this phenomenon is ubiquitous. Although of very low amplitude, the period doubling subharmonics can also be detected in ground-based data of sufficiently good quality (Netzel et al. 2015b). Not surprisingly then, we have found subharmonics also in EPIC 201585823, which we discuss in Sections 2.4 and 2.5.

Multimode pulsation promises better asteroseismic information on the stellar structure of RR Lyr stars, hence deeper understanding both of stellar pulsation and of the interior properties of these important distance indicators. Asteroseismology depends on modelling identified mode frequencies (Aerts, Christensen-Dalsgaard & Kurtz 2010), hence more frequencies give better constraints on models. In this paper, we announce the discovery of a new triple-mode RR Lyr star, EPIC 201585823, that is remarkably similar to 11 other triple-mode RR Lyr stars. We also compare and discuss several data reduction pipelines and other rectifications of *Kepler* K2 mission data.

## 2 THE TRIPLE MODE RR LYR STAR EPIC 201585823

### 2.1 Data

The data for EPIC 201585823 were obtained during Campaign 1 (C1) of the *Kepler* two-reaction-wheel extended mission, known as the K2 mission (Howell et al. 2014). Several independent reductions

<sup>1</sup> OGLE is the Optical Gravitational Lensing Experiment studying the Galactic bulge and the Magellanic Clouds. For general information on the OGLE-III and OGLE-IV surveys, see Udalski et al. (2008) and Udalski, Szymański & Szymański (2015), for specific studies of RR Lyr stars in the Galactic Bulge, see Soszyński et al. (2011) and Soszyński et al. (2014).

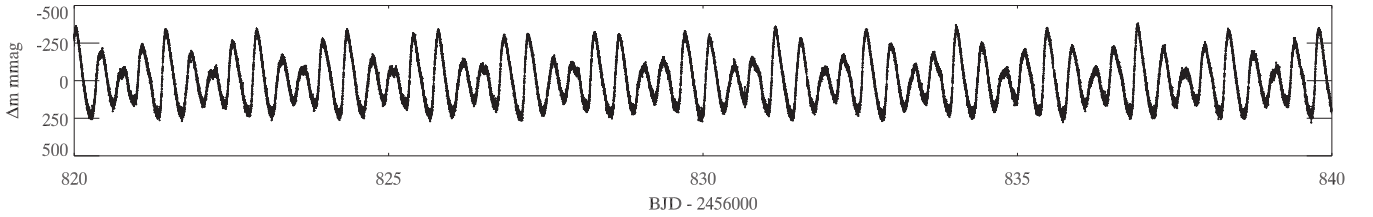


**Figure 1.** A section of the K2P<sup>2</sup> SC raw light curve of EPIC 201585823 spanning 20 d showing the high-amplitude light variations. Almost all of the variation in the light curve is explained by the non-linear interaction of the fundamental and first-overtone radial p modes in this RRd star.

and rectifications of the data are available publicly, and we compare these in Section 3 below. The K2 mission observes fields in the ecliptic plane where the two operational reaction wheels, balanced against solar radiation pressure, provide some pointing stability. Nevertheless, there is drift in the position of the satellite that must be corrected with thruster bursts on time-scales of 5.9 h (or multiples of that) and there are reaction wheel resaturations every 2 d (Howell et al. 2014; Vanderburg & Johnson 2014). These drifts plus thruster corrections can produce abrupt changes in the measured flux that must be corrected or ameliorated to obtain photometric noise levels of the order of 2–4 times greater than those for the original *Kepler* mission, where pointing with three reaction wheels was stable to a small fraction of a pixel.

Vanderburg & Johnson (2014), Armstrong et al. (2015) and Lund et al. (2015) have devised pipelines to create improved pixel masks and/or to correct for pointing drift for each star in the K2 campaign fields. These pipelines are not equivalent, and the results are dependent on the variability in the stars. RR Lyr stars, for example, typically have periods of the order of 12 h (less than 0.5 d for RRc stars and greater than 0.5 d for RRab stars), with rapid increases in brightness followed by a slower decrease (RRab stars), or a more sinusoidal variation in the case of RRc stars. The amplitudes are relatively large – several tenths of a magnitude to well over 1 mag – so that the rise and fall times of the light variation are similar to the 5.9 h thruster firing schedule of the K2 mission. This can lead to overcorrection of the instrumental slopes of the light curves of RR Lyr stars, so care must be taken when using pipeline data for these stars, and when creating custom data rectification, either automatically or by hand.

For EPIC 201585823, we have examined and compared the pipeline reductions and show the results in Section 3 below. A consequence of the large amplitude of EPIC 201585823 and its pulsation time-scale resonating with the thruster firing times leads to pipeline-corrected light curves that sometimes are more non-sinusoidal, hence with more combination frequency peaks, than in ‘raw’ data that have been extracted with a customised mask and corrected for flat-field and cosmic ray exclusion, but not corrected for changes in the satellite pointing. Thus, for the astrophysical analysis of this star we have chosen to use ‘raw’ data extracted by us as part of the K2P<sup>2</sup> pipeline (K2-Pixel-Photometry; Lund et al. 2015).<sup>2</sup> This may be the preferred choice for analysis of RR Lyr stars from K2 data. The K2P<sup>2</sup> pipeline automatically creates a mask that encompasses all pixels with significant signal for a star by using a summed image for mask selection. This therefore encompasses the approximately 1 pixel drift between the 5.9 h thruster firings. The mask we used is shown in comparison with those of other pipelines in Section 3.

<sup>2</sup> Available from the *Kepler* Asteroseismic Science Operations Centre; <http://kasoc.phys.au.dk>

## 2.2 Frequency analysis of the K2P<sup>2</sup> SC raw light curve

The K2P<sup>2</sup> ‘raw’ short cadence (SC; 58.9 s integrations) data were analysed for their component frequencies. These data were obtained using a pipeline-generated mask encompassing all pixels with significant signal for the star, were flat-fielded, and had outliers removed, particularly at the times of thruster firings. They were not corrected for instrumental variations caused by pointing drift and re-setting, for reasons given in Section 2.1 above. The data set consists of 112 545 points spanning 80.1 d. Fig. 1 shows a typical 20 d section of the light curve where the variations, dominated by the fundamental and first-overtone radial modes, can be seen. Note that the light curve is non-linear, with larger ‘upward’ than ‘downward’ excursions about the mean. We explain that upward light curve shape in Section 2.6 below, following Kurtz et al. (2015).

We performed a frequency analysis on the EPIC 201585823 K2 C1 K2P<sup>2</sup> raw SC data set. We used the interactive light curve and amplitude spectrum tools in the program PERIOD04 (Lenz & Breger 2004). We then used a discrete Fourier transform (Kurtz 1985) and our own least-squares and non-linear least-squares fitting programs to find the frequencies, amplitudes and phases to describe the light curves. After setting the mean of the data set to zero, we fitted a cosine function,  $\Delta m = A \cos(2\pi f(t - t_0) + \phi)$ , for each frequency in the data in magnitudes, thus defining our convention for the phases in this paper. The zero-point of the time-scale for the phases is BJD 2 456850.30000. Our routines and PERIOD04 are in agreement.

## 2.3 The fundamental and first-overtone radial modes

The light variations of EPIC 201585823 are dominated by two peaks in the amplitude spectrum, which we identify as the fundamental and first-overtone radial modes from their period ratio, and that can be seen in the top panel of Fig. 2. We identified the two highest peaks and fitted them by linear and non-linear least-squares to the data with the results shown in Table 1. For generality, we label the fundamental radial mode frequency  $\nu_1$ , and the first-overtone radial mode frequency  $\nu_2$ . Traditionally in studies of RR Lyr stars these are called  $f_0$  and  $f_1$ , respectively, or ‘F’ and ‘1O’, for the fundamental and first-overtone radial modes. The period ratio,  $0.744\,770 \pm 0.000\,003$ , is consistent with other RRd stars, and with RR Lyr star models for fundamental and first-overtone radial pulsation. The error in amplitude is estimated to be  $1\sigma = 0.07$  mmag from the fit of the two base frequencies and their combination terms as seen in Table 2. The frequency errors and phase errors are proportional to the amplitude error (Montgomery & O’Donoghue 1999), hence are scaled appropriately.

Pulsations in RR Lyr stars, including RRd stars, are known to be non-sinusoidal, with many harmonics and combination frequencies (see e.g. Jerzykiewicz & Wenzel 1977; Chadid 2012). We therefore searched for combination frequencies for  $\nu_1$  and  $\nu_2$  up to terms of order  $5\nu$ . While combination frequency peaks with terms higher

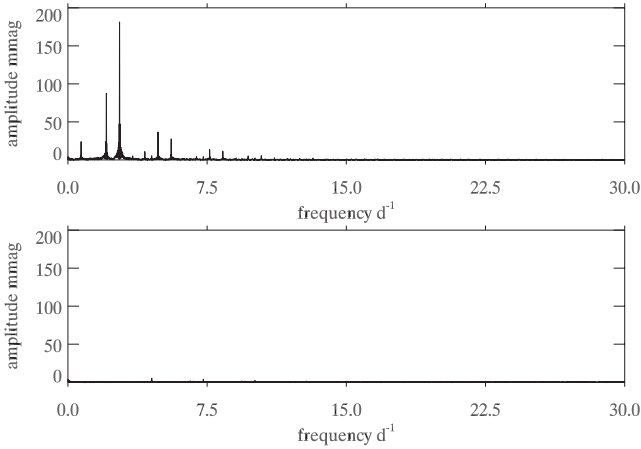


**Figure 2.** Top: an amplitude spectrum of the *Kepler* K2 C1 raw SC data for EPIC 201585823 out to  $30 \text{ d}^{-1}$ . The two highest amplitude peaks,  $\nu_1$  and  $\nu_2$ , are generated by the principal pulsation modes, which we identify as the fundamental and first-overtone radial modes based on their period ratio of 0.745. Most of the other peaks seen in this panel are combination frequencies. Bottom panel: after pre-whitening by  $\nu_1$ ,  $\nu_2$  and 42 combination frequencies up to order  $5\nu$  and with amplitudes greater than  $0.15 \text{ mmag}$ . This plot has been kept on the same ordinate scale as the top panel to make clear that most of the variance is in the two non-linearly interacting radial modes. There is significant variance left that is shown below with this panel at a higher ordinate scale in Fig. 3.

**Table 1.** A non-linear least-squares fit of only the two principal pulsation mode frequencies of EPIC 201585823, identified with the radial fundamental ( $f_0$ ) and first-overtone ( $f_1$ ) modes. The zero-point of the time-scale for the phases is BJD 2 456850.30000.

Labels	Frequency ( $\text{d}^{-1}$ )	Amplitude (mmag) $\pm 0.07$	Phase radians
$\nu_1$ ( $f_0$ )	$2.072\,143 \pm 0.000\,005$	88.34	$1.1525 \pm 0.0008$
$\nu_2$ ( $f_1$ )	$2.782\,259 \pm 0.000\,003$	181.70	$-2.1659 \pm 0.0004$

than  $5\nu$  are identifiable in K2 data for this star at amplitudes higher than our  $0.15 \text{ mmag}$  cutoff, we chose not to include higher order terms to keep the number of combination frequencies low for convenience of visualization, and to avoid chance coincidences of combination frequencies with each other, and with peaks near the noise level. This does mean that some combination frequency peaks with amplitudes greater than  $0.15 \text{ mmag}$  remain in our amplitude spectra.

We did not search the amplitude spectrum for significant peaks that were then identified with combination frequencies. Instead, we hypothesized a combination frequency model and calculated the exact values of the combination frequencies from the base frequencies,  $\nu_1$  and  $\nu_2$ , given in Table 1; we then fitted the base frequencies and their combinations to the data by linear least-squares. This generated 42 combination frequencies, in addition to the two base frequencies, with amplitudes greater than or equal to  $0.15 \text{ mmag}$  ( $2\sigma$  of our amplitude error); we discarded a further 16 combination frequencies with amplitudes lower than this limit. We then fitted the adopted 44 frequencies by linear least-squares to the data; the results are listed in Table 2.

**Table 2.** A linear least-squares fit of the two principal pulsation mode frequencies of EPIC 201585823, identified with the radial fundamental and first-overtone modes, plus 42 combination frequencies up to order  $5\nu$  and with amplitudes greater than  $0.15 \text{ mmag}$ . The zero-point of the time-scale for the phases is BJD 2 456850.30000.

Labels	Frequency ( $\text{d}^{-1}$ )	Amplitude (mmag) $\pm 0.07$	Phase radians
$-4\nu_1 + 3\nu_2$	0.058 205	1.45	$-0.8924 \pm 0.0498$
$3\nu_1 - 2\nu_2$	0.651 911	0.30	$-0.7876 \pm 0.2441$
$-\nu_1 + \nu_2$	0.710 116	24.09	$0.6326 \pm 0.0031$
$-5\nu_1 + 4\nu_2$	0.768 321	0.38	$-3.0419 \pm 0.1966$
$2\nu_1 - \nu_2$	1.362 027	1.75	$-0.2407 \pm 0.0421$
$-2\nu_1 + 2\nu_2$	1.420 232	1.80	$-0.1891 \pm 0.0409$
$5\nu_1 - 3\nu_2$	2.013 938	0.15	$-2.7546 \pm 0.4799$
$\nu_1$	2.072 143	88.43	$1.1525 \pm 0.0008$
$-3\nu_1 + 3\nu_2$	2.130 348	0.31	$0.3009 \pm 0.2353$
$\nu_2$	2.782 259	181.64	$-2.1657 \pm 0.0004$
$3\nu_1 - \nu_2$	3.434 170	0.39	$-0.3131 \pm 0.1890$
$-\nu_1 + 2\nu_2$	3.492 375	4.68	$2.9487 \pm 0.0158$
$-5\nu_1 + 5\nu_2$	3.550 580	0.21	$-2.4231 \pm 0.3502$
$2\nu_1$	4.144 286	11.14	$-0.0980 \pm 0.0066$
$-2\nu_1 + 3\nu_2$	4.202 491	0.93	$0.6101 \pm 0.0792$
$\nu_1 + \nu_2$	4.854 402	36.89	$3.1205 \pm 0.0020$
$2\nu_2$	5.564 518	27.85	$0.5041 \pm 0.0026$
$3\nu_1$	6.216 429	1.29	$-0.6625 \pm 0.0572$
$-\nu_1 + 3\nu_2$	6.274 634	2.05	$2.2999 \pm 0.0359$
$2\nu_1 + \nu_2$	6.926 545	4.86	$2.2648 \pm 0.0152$
$-2\nu_1 + 4\nu_2$	6.984 750	0.84	$2.1840 \pm 0.0877$
$\nu_1 + 2\nu_2$	7.636 661	13.81	$-1.0229 \pm 0.0053$
$-3\nu_1 + 5\nu_2$	7.694 866	0.21	$0.8220 \pm 0.3556$
$3\nu_2$	8.346 777	11.76	$2.9695 \pm 0.0063$
$3\nu_1 + \nu_2$	8.998 688	1.13	$0.8866 \pm 0.0653$
$-\nu_1 + 4\nu_2$	9.056 893	1.86	$-2.4803 \pm 0.0397$
$2\nu_1 + 2\nu_2$	9.708 804	5.08	$-1.5072 \pm 0.0145$
$-2\nu_1 + 5\nu_2$	9.767 009	0.65	$-2.1820 \pm 0.1136$
$\nu_1 + 3\nu_2$	10.418 920	5.57	$2.4194 \pm 0.0132$
$4\nu_1 + \nu_2$	11.070 831	0.30	$1.5387 \pm 0.2462$
$4\nu_2$	11.129 036	2.86	$-0.3051 \pm 0.0258$
$3\nu_1 + 2\nu_2$	11.780 947	0.72	$-1.6379 \pm 0.1027$
$-\nu_1 + 5\nu_2$	11.839 152	1.27	$0.1206 \pm 0.0580$
$2\nu_1 + 3\nu_2$	12.491 063	1.51	$1.5338 \pm 0.0488$
$\nu_1 + 4\nu_2$	13.201 179	2.18	$-0.9836 \pm 0.0339$
$5\nu_2$	13.911 295	1.26	$2.9376 \pm 0.0583$
$3\nu_1 + 3\nu_2$	14.563 206	0.21	$0.2337 \pm 0.3578$
$2\nu_1 + 4\nu_2$	15.273 322	0.77	$-2.4566 \pm 0.0953$
$5\nu_1 + 2\nu_2$	15.925 233	0.15	$-0.0189 \pm 0.4893$
$\nu_1 + 5\nu_2$	15.983 438	1.11	$1.7042 \pm 0.0663$
$3\nu_1 + 4\nu_2$	17.345 465	0.41	$3.1159 \pm 0.1795$
$2\nu_1 + 5\nu_2$	18.055 581	0.51	$0.5658 \pm 0.1439$
$5\nu_1 + 3\nu_2$	18.707 492	0.20	$-1.9411 \pm 0.3752$
$3\nu_1 + 5\nu_2$	20.127 724	0.21	$-0.1201 \pm 0.3580$

Pre-whitening the data by the 44 frequencies given in Table 2 results in the amplitude spectrum shown in the bottom panel of Fig. 2. This has intentionally been kept on the same ordinate scale as the top panel of the figure for impact: most of the variance is in the fundamental and first-overtone radial mode frequencies, and their combination frequencies, as is typical of RRd stars. However, with a higher ordinate scale there are many real peaks still to be examined, as we discuss in detail next in Section 2.4 and show in Fig. 3.



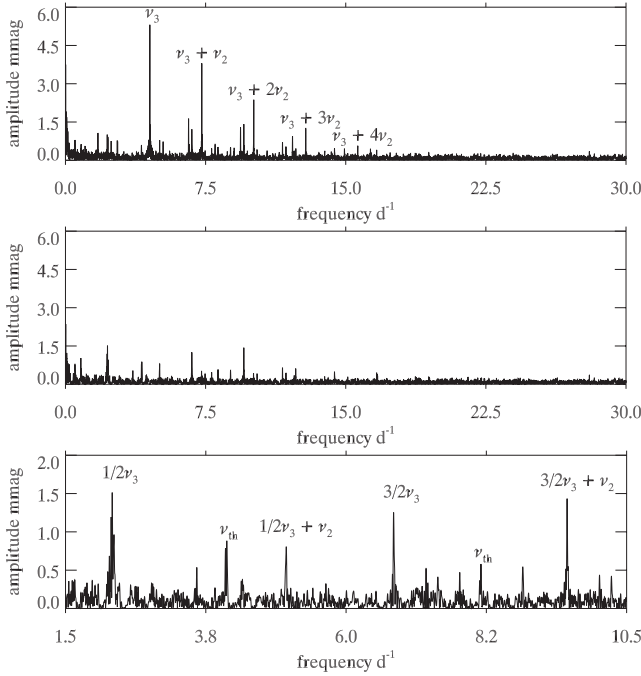


**Figure 3.** Top: the same amplitude spectrum as in the bottom panel of Fig. 2 after pre-whitening by  $\nu_1$ ,  $\nu_2$  and 42 combination frequencies up to order  $5\nu$  and with amplitudes greater than 0.15 mmag, but on a larger scale. The highest peak is  $\nu_3 = 4.51456 \text{ d}^{-1}$ . Four combination frequencies with  $\nu_2$  are labelled, indicating that  $\nu_3$  is a mode frequency. Middle: the amplitude spectrum of the residuals to a 414 frequency fit with  $\nu_1$ ,  $\nu_2$  and  $\nu_3$ , plus combination frequencies up to order  $5\nu$  and with amplitudes greater than or equal to 0.15 mmag. Bottom: an expanded look at the middle panel showing the subharmonics of  $\nu_3$ . For clarity, combination peaks of the subharmonics with  $\nu_2$  with relatively high amplitude are marked. Two frequencies are marked as  $\nu_{th}$ ; these are artefacts at the thruster frequency,  $4.08 \text{ d}^{-1}$ , and its harmonic,  $8.16 \text{ d}^{-1}$ . Multiple peaks are seen for those, since the thruster firings are not purely periodic. These artefacts, and higher harmonics of the thruster firing frequency are common in K2 data sets.

#### 2.4 A third mode frequency – a non-radial mode

After pre-whitening by  $\nu_1$ ,  $\nu_2$  and their 42 combination terms listed in Table 2 we find a third frequency,  $\nu_3 = 4.51456 \pm 0.00008 \text{ d}^{-1}$ , which has a number of combination frequencies with  $\nu_1$  and  $\nu_2$ , many of which are evident in the top panel of Fig. 3 (which is the same as the bottom panel of Fig. 2, but with higher ordinate scale). The four highest amplitude combination frequencies with  $\nu_2$  are marked, and others can be seen. That  $\nu_3$  couples to  $\nu_1$  and  $\nu_2$  argues that it is a mode frequency. It does not coincide with any combination frequency of  $\nu_1$  and  $\nu_2$ .

A non-linear least-squares fit of  $\nu_1$ ,  $\nu_2$  and  $\nu_3$  is given in Table 3 (but not their 411 combination frequencies with amplitudes greater than or equal to 0.15 mmag, which are too numerous to list). From this we associate  $\nu_3$  with a non-radial pulsation mode, based on its period ratio with the highest amplitude mode, the first-overtone radial mode at  $\nu_2$ ; this ratio is  $0.616285 \pm 0.000012$ .

This is similar to the period ratios that were found in 11 other triple-mode RRd stars, which are listed in Table 4, and in 260 double mode RRc stars that pulsate in the first-overtone radial mode and an addition non-radial mode (for lists of those stars see: Jurcsik et al. 2015; Moskalik et al. 2015; Netzel et al. 2015a,b). We thus conclude that EPIC 201585823 is a new member of a (currently) rare class of triple-mode RR Lyr stars.

**Table 3.** A non-linear least-squares fit of the two principal pulsation mode frequencies of EPIC 201585823, identified with the radial fundamental ( $f_0$ ) and first-overtone ( $f_1$ ) modes, and the third mode frequency  $\nu_3$ , which arises from a non-radial mode. The zero-point of the time-scale for the phases is BJD 2 456850.30000.

Labels	Frequency ( $\text{d}^{-1}$ )	Amplitude (mmag) $\pm 0.07$	Phase radians
$\nu_1 (f_0)$	$2.072142 \pm 0.000005$	88.34	$1.1525 \pm 0.0008$
$\nu_2 (f_1)$	$2.782258 \pm 0.000003$	181.70	$-2.1659 \pm 0.0004$
$\nu_3$	$4.514560 \pm 0.000080$	5.60	$-0.5938 \pm 0.0125$

To show the similarity of these triple-mode RR Lyr stars more specifically, in Table 5 we compare the three mode frequencies of EPIC 201585823 with those of V87 in M3 (Jurcsik et al. 2015). The frequencies are very similar in these two stars, as they are also similar to those of the triple-mode RR Lyr variables V68 in M3 (Jurcsik et al. 2015) and CoRoT 101368812 (Chadid 2012). These four triple-mode pulsators seem to be of similar stellar structure, hence in similar evolutionary states. In the other known stars of this type, frequencies of the modes are different, yet their ratios are still almost the same. In particular, the period ratio of the non-radial mode to the first-overtone radial mode is always in a narrow range of 0.611–0.621. It will be interesting to see whether other triple-mode RR Lyr stars that are found in the future will also show such similarity. Many RR Lyr stars are being observed in the K2 campaign fields,<sup>3</sup> and it is reasonable to expect the discovery of more triple-mode RR Lyr variables.

After fitting  $\nu_1$ ,  $\nu_2$ ,  $\nu_3$  and combination frequencies to the data and pre-whitening, the middle and bottom panels of Fig. 3 show the amplitude spectrum of the residuals. Six peaks are marked: two are very close to the exact subharmonics of  $\nu_3$  at  $\frac{1}{2}\nu_3$  and  $\frac{3}{2}\nu_3$ ; two are combination frequencies between the subharmonics and  $\nu_2$  at  $\frac{1}{2}\nu_3 + \nu_2$  and  $\frac{3}{2}\nu_3 + \nu_2$ ; and two, marked as  $\nu_{th}$ , are artefacts at the thruster firing frequency and its harmonic.

In table 8 of Moskalik et al. (2015), there are 13 stars (four RRd and nine RRc) with space photometry. Subharmonics were detected in all four RRd stars and in six of the nine RRc stars. Thus, with space photometry these subharmonics are found in most RRc and RRd stars, and their properties are found to be the same in RRc and in RRd stars. These subharmonics can also be detected in ground-based studies. In the OGLE-IV Galactic bulge survey data, Netzel et al. (2015b) found 131 RRc stars with period ratios near 0.61. Of those, 26 showed a subharmonic at  $\frac{1}{2}\nu$  of the non-radial mode frequency, and two more showed a subharmonic at  $\frac{3}{2}\nu$ .

Subharmonics are indicative of period doubling, and in EPIC 201585823 they show unresolved, broad frequency peaks, which have also been seen in other stars showing the  $\nu_3$  mode frequency; this shows that the period doubling changes are not constant in time (Moskalik et al. 2015). We examine the frequency and/or amplitude changes of  $\nu_3$  further in Section 2.5 below. The values of the subharmonics,  $\frac{1}{2}\nu_3$  and  $\frac{3}{2}\nu_3$ , are not well determined from the full data set. Their frequency and amplitude variability give rise to asymmetric and multiple peaks in the amplitude spectrum, as can be seen in the bottom panel of Fig. 3. Selecting the highest peak in both cases gives formal values of  $\frac{1}{2}\nu_3 = 2.2492 \pm 0.0003 \text{ d}^{-1}$  and

<sup>3</sup> <http://keplergo.github.io/KeplerScienceWebsite/k2-approved-programs.html> lists approved programmes for K2.

**Table 4.** A list of the 12 known triple-mode RR Lyrae stars with period ratios near 0.61. The stars are ordered by increasing  $P_2$ , the period for the dominant first-overtone radial mode.  $P_3/P_2$  is the ratio of the non-radial mode period ( $P_3$ ) to that of the radial first overtone. All stars are remarkably similar in their period ratios.

Name	$P_1$ (d)	$P_2$ (d)	$P_3$ (d)	$P_3/P_2$	Reference
OGLE-BLG-RRLYR-02027	0.3799	0.2786	0.1702	0.6107	Netzel et al. (2015a)
OGLE-BLG-RRLYR-07393 <sup>a</sup>	0.4627	0.3449	0.2126	0.6163	Smolec et al. (2015a)
V125 in M3	0.4709	0.3498	0.2158	0.6168	Jurcsik et al. (2015)
V13 in M3 <sup>a, b</sup>	0.4795	0.3507	0.2153	0.6137	Jurcsik et al. (2015)
V68 in M3	0.4785	0.3560	0.2187	0.6145	Jurcsik et al. (2015)
V87 in M3	0.4802	0.3575	0.2208	0.6177	Jurcsik et al. (2015)
EPIC 201585823	0.4826	0.3594	0.2215	0.6163	This paper
CoRoT 101368812	0.4880	0.3636	0.2233	0.6141	Chadid (2012)
EPIC 60018653	0.5394	0.4023	0.2479	0.6162	Molnár et al. (2015)
AQ Leo	0.5498	0.4101	0.2547	0.6211	Gruberbauer et al. (2007)
EPIC 60018662	0.5590	0.4175	0.2574	0.6166	Molnár et al. (2015)
OGLE-BLG-RRLYR-14031	0.5761	0.4298	0.2647	0.6159	Netzel et al. (2015a)

Notes. <sup>a</sup>Blazhko modulation of dominant radial modes; <sup>b</sup>weak radial second overtone detected.

**Table 5.** A comparison of the mode frequencies for EPIC 201585823 and V87 in M3 (Jurcsik et al. 2015). The stars are remarkably similar.

	EPIC 201585823		V87 in M3		
	Frequency (d <sup>-1</sup> )	Amplitude (mmag)	Frequency (d <sup>-1</sup> )	Amplitude (mmag)	Frequency ratio
$\nu_1$	2.072 142	88.3	2.082 60	110.0	1.005
$\nu_2$	2.782 258	181.7	2.797 28	230.0	1.005
$\nu_3$	4.514 560	5.6	4.528 80	7.8	1.003

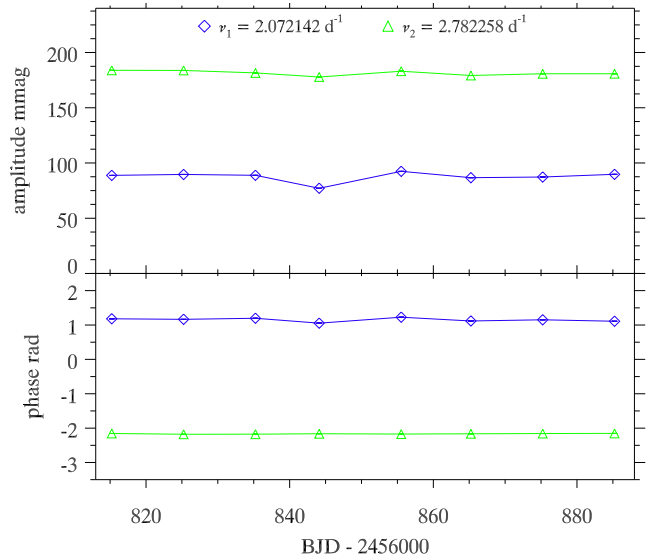
$\frac{3}{2}\nu_3 = 6.7625 \pm 0.0004$  d<sup>-1</sup>; these are nominally just resolved from the exact half integer values of 2.2573 and 6.7718 d<sup>-1</sup>, respectively.

While there are further significant peaks seen in the bottom panel of Fig. 3, we chose to terminate the frequency analysis at this point, leaving the question of whether these other peaks belong to other pulsation modes, combination frequencies, instrumental artefacts or other variations in the data. Our caution arises from the difficulty of rectifying fully the K2 data for RR Lyr stars. We illustrate some of the problems with that in Section 3 below.

## 2.5 Frequency and amplitude variability

We employed the methodology of Bowman & Kurtz (2014), who tracked amplitude and phase at fixed frequency through a series of discrete time bins to study variable pulsation amplitudes and frequencies in a  $\delta$  Sct star, KIC 7106205. For EPIC 201585823, we used the frequencies given in Table 3, which were determined from the entire 80.1 d data set. We then divided the data set into eight bins, each 10 d in length. Values of amplitude and phase were optimized at fixed frequency using linear least-squares in each time bin and plotted against time. The results are shown in Fig. 4 for  $\nu_1$  and  $\nu_2$ , and in the left-hand panel of Fig. 5 for  $\nu_3$ . The zero-point of the time-scale for the phases is BJD 2 456 850.30000. We chose to study the observed phase variation by keeping the frequency fixed in a linear least-squares fit, which is equivalent to studying frequency variation at fixed phase.

The radial fundamental and first-overtone mode frequencies,  $\nu_1$  and  $\nu_2$ , are shown in Fig. 4. They exhibit little amplitude or phase variation over the 80.1 d of K2 observations. In the absence of the Blazhko effect, for which we have no clear evidence in this star, this result is not unexpected for high-amplitude, low-order radial p modes. Non-Blazhko RR Lyr stars have stable frequencies and

**Figure 4.** Tracking plot showing optimized values of amplitude and phase at fixed frequency using linear least-squares in 10 d bins for the fundamental mode frequency  $\nu_1$  and the radial first-overtone mode frequency  $\nu_2$ .  $1\sigma$  error bars calculated from the least-squares fit are plotted, but are generally smaller than the data points. The zero-point of the time-scale for the phases is BJD 2 456 850.30000.

amplitudes over this time span; typical changes in frequency of radial modes are of the order of less than 0.01 per cent (e.g. Jurcsik et al. 2015). There is a small drop in amplitude in the middle of the observations (approximately BJD 2 456 845) for both  $\nu_1$  and  $\nu_2$  in Fig. 4; this may be instrumental in origin since that bin contains a gap in the observations.

The third frequency  $\nu_3$  (shown in the left-hand panel of Fig. 5) and its subharmonics  $\frac{1}{2}\nu_3$  and  $\frac{3}{2}\nu_3$  (shown in the right-hand panel of Fig. 5), exhibit considerable amplitude and phase variation over 80.1 d. This behaviour is the same as that seen in RRc stars using similar techniques reported by Moskalik et al. (2015, their figs 6 and 7), Szabó et al. (2014, their fig. 11) and Molnár et al. (2015, their fig. 5). We conclude that the non-radial mode in these stars commonly shows amplitude and frequency variability.

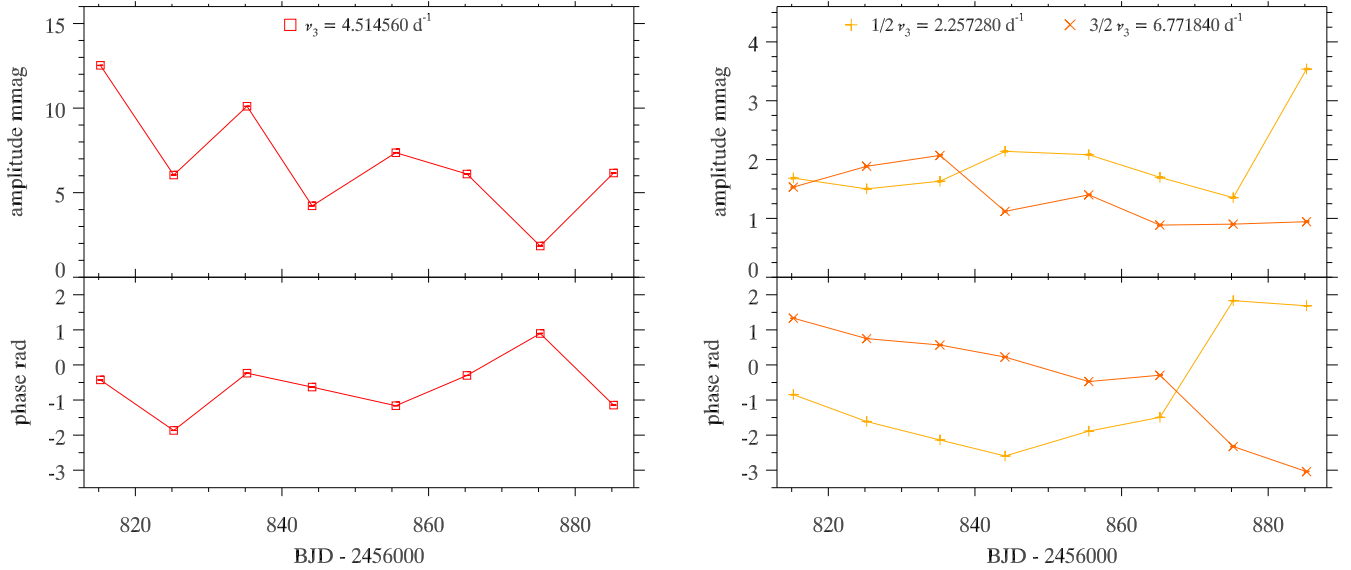


**Figure 5.** Tracking plots showing optimized values of amplitude and phase at fixed frequency using linear least-squares in 10 d bins. Left-hand panel: the non-radial mode frequency  $\nu_3$ . Right-hand panel: subharmonics of  $\nu_3$ .  $1\sigma$  error bars are plotted as calculated from the least-squares fit; they are generally smaller than the data points. The zero-point of the time-scale for the phases is BJD 2 456 850.30000. Both the amplitudes and the phases (thus frequencies) are variable.

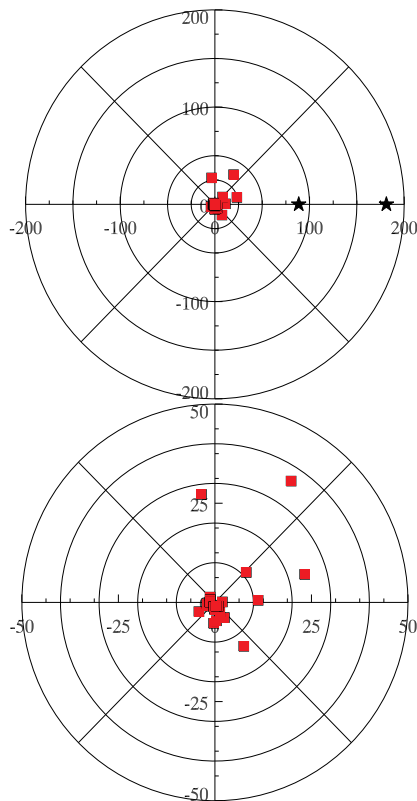


**Figure 6.** Phasor plots for EPIC 201585823. These polar plots show amplitude in mmag as the radial coordinate and phase in radians as the angular coordinate. The relative phase is defined as  $\phi_r = \phi_{\text{obs}} - \phi_{\text{calc}} = \phi_{\text{obs}} - (n\phi_1 + m\phi_2)$ . The convention is such that upward shaped light curves have combination frequency phases near to zero phase in the right-hand section of the diagrams (Kurtz et al. 2015). The top panel shows the amplitudes of the base frequencies (black stars),  $\nu_1$  and  $\nu_2$ , with their phases set to zero. Because of the large relative amplitudes of the base frequencies compared to the combination frequencies, the bottom plot shows those combination frequency amplitudes and phases at a larger scale.

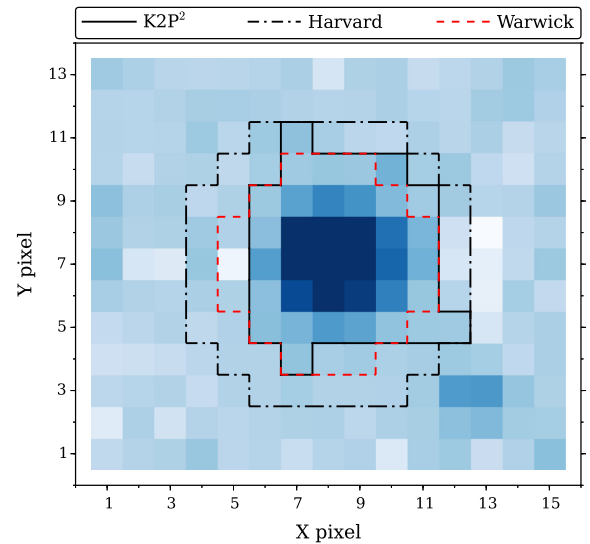


**Figure 7.** Pixel masks adopted for EPIC 20158523 for the different pipelines used in this work (see legend). The colours depict the summed image with the background subtracted from individual frames (see Lund et al. 2015); the colour scale is logarithmic and goes from light (low flux) to dark blue (high flux). For the Harvard and Warwick pipelines we show the masks obtained from the MAST data. The faint target in the lower-right part of the plot, centred on pixel (13,3), was also detected by the K2P² pipeline but we have omitted its mask in this plot.

## 2.6 Phasor plots for the radial modes

Kurtz et al. (2015) showed that the shapes of the light curves of strongly non-linearly pulsating Slowly Pulsating B stars and  $\gamma$  Dor stars are governed by the phases of the combination frequencies. In particular, light curves with an ‘upward’ shape, such as that seen for EPIC 201585823 in Fig. 1, are the result of combination frequencies having phases close to zero in comparison with the base frequencies. We show that is the case for EPIC 201585823 in Fig. 6, where the highest amplitude combination frequencies of  $\nu_1$



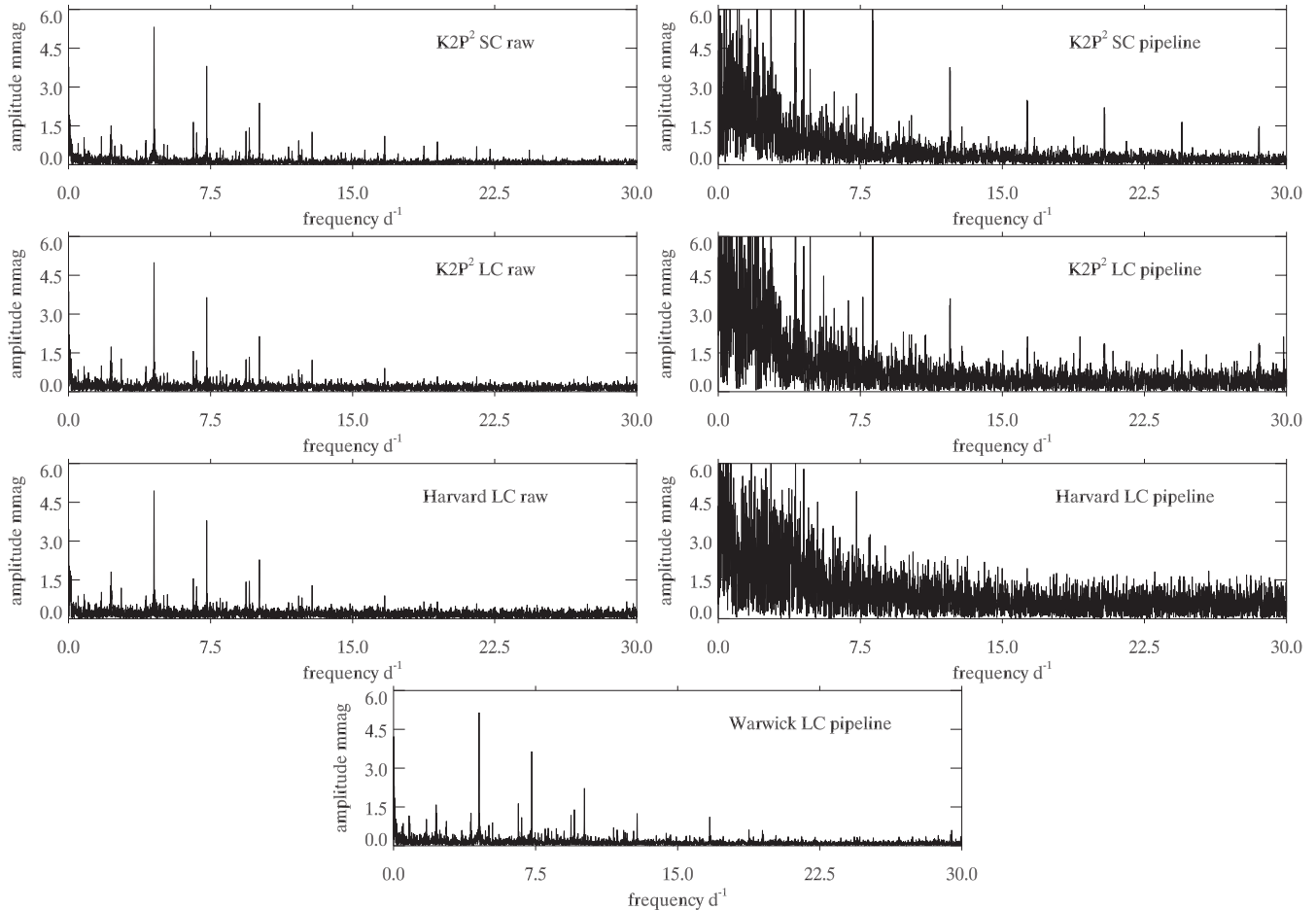


**Figure 8.** This diagram compares the amplitude spectra of the residuals to the 44-frequency fit given in Table 2 for different data reductions. Left-hand column and bottom centre: these compare the raw data and the Warwick pipeline, which give similar results. Right-hand column and bottom centre: these compare the various pipeline reductions: K2P<sup>2</sup> SC and LC pipeline data (Handberg & Lund 2014; Lund et al. 2015), Harvard LC pipeline data (Vanderburg & Johnson 2014) and Warwick LC pipeline data (Armstrong et al. 2015). The highest peak is  $\nu_3$ ; immediately to its left is the  $<1$  mmag thruster firing artefact at  $4.09 \text{ d}^{-1}$ , for comparison. The relatively high noise at low frequency in some of the pipeline data is a consequence of the high amplitude of the RR Lyr programme star; it is not indicative of the quality of the pipelines for more tractable light curves.

and  $\nu_2$  (see Table 2) lie to the right with relative phases near zero, as expected for an upward light curve.

The upward non-linearity of the RR Lyr light curves has previously been considered to be normal and understood. That the relative phases of the combination frequencies to those of the base mode frequencies in these stars are as predicted by Kurtz et al. (2015) supports their interpretation of upward and downward non-linearities in pulsating star light curves in general.

### 3 A COMPARISON OF THE DIFFERENT PIPELINES

The analysis of EPIC 201585823 in this paper used K2P<sup>2</sup> SC ‘raw’ data with a pipeline created mask to capture all pixels with significant variability, corrected for flat-field and removed obvious outliers. Fig. 7 shows the mask we used in comparison with the masks used by Vanderburg & Johnson (2014) and Armstrong et al. (2015). We did not correct for the pointing changes caused by drift and thruster firings, nor for possible other long-term trends.

We compared the amplitude spectra of the residuals to the 44-frequency fit for K2P<sup>2</sup> SC and LC raw and pipeline data (Handberg & Lund 2014; Lund et al. 2015), Harvard LC raw and pipeline

data (Vanderburg & Johnson 2014) and Warwick LC pipeline data (Armstrong et al. 2015) with results seen in Fig. 8. It is clear that some pipeline data have increased low-frequency noise as a result of the time-scale of the rise and fall of the RR Lyr light curve being close to the 5.9 h thruster firing time-scale, making it difficult to separate the stellar and instrumental variations. In this case, it is preferable not to model the pointing corrections. We also do not recommend a hands-on correction segment-by-segment, either by eye or with, say, polynomial fits, because this has as its basis a mental model that is necessarily subjective and not reproducible by other investigators. For the K2 RR Lyr stars, we therefore recommend carefully chosen masks (either automatic or custom), flat-fielding and outlier removal, but no corrections for the pointing changes; that is, the use of what we call ‘raw’ data.

### 4 CONCLUSIONS

We have discovered a new, rare triple-mode RR Lyr star, EPIC 201585823, in the *Kepler* K2 mission C1 data. This star pulsates primarily in the fundamental and first-overtone radial modes, and, in addition, a third non-radial mode. The ratio of the period of the non-radial mode to that of the first-overtone radial mode,

0.616 285, is remarkably similar to that seen in 11 other triple-mode RR Lyr stars, and in 260 RRc stars observed in the Galactic bulge. There are 10 RRc stars observed from space (Moskalik et al. 2015) and nine of them show the non-radial mode with the 0.61 period ratio. The number of similar RRc and RRd stars observed from the ground is growing rapidly. With further high-precision space data and large-scale ground-based studies these behaviours will be seen to be normal in many RR Lyr stars. This systematic character promises new constraints on RR Lyr star models.

We detected subharmonics of the non-radial mode frequency, which are a signature of period doubling of this oscillation; we note that this phenomenon is ubiquitous in RRc and RRd stars observed from space, and from ground with sufficient precision. The non-radial mode and subharmonic frequencies are not constant in frequency or in amplitude.

The amplitude spectrum of EPIC 201585823 is dominated by many combination frequencies among the three interacting pulsation mode frequencies. Inspection of the phase relationships of the combination frequencies in a phasor plot explains the ‘upward’ shape of the light curve.

We found that raw data with custom masks encompassing all pixels with significant signal for the star, but without correction for pointing changes, is best for frequency analysis of this star, and, by implication, other RR Lyr stars observed by the K2 mission.

## ACKNOWLEDGEMENTS

Some/all of the data presented in this paper were obtained from the Mikulski Archive for Space Telescopes (MAST). STScI is operated by the Association of Universities for Research in Astronomy, Inc., under NASA contract NAS5-26555. Support for MAST for non-HST data is provided by the NASA Office of Space Science via grant NNX09AF08G and by other grants and contracts. This work has used data for EPIC\201585823, which is one of the K2 targets selected and proposed by the RR\Lyrae and Cepheid Working Group of the Kepler Asteroseismic Science Consortium (proposal number GO1067). We thank Dr David Armstrong for discussion concerning the Warwick pipeline data, and Dr Simon Murphy for discussion concerning the phasor plots. DWK and DMB are funded by the UK STFC. SJE was supported during this research by a University of Central Lancashire Undergraduate Research Internship. PM is supported by the Polish National Science Center through grant DEC-2012/05/B/ST9/03932. RH and MNL are supported by funding to the Stellar Astrophysics Centre at Aarhus University provided by the Danish National Research Foundation (Grant DNRF106), and by the ASTERISK project (ASTERoseismic Investigations with SONG and Kepler) funded by the European Research Council (grant agreement no.: 267864).

## REFERENCES

Aerts C., Christensen-Dalsgaard J., Kurtz D. W., 2010, *Asteroseismology*. Springer-Verlag, Netherlands

- Armstrong D. J. et al., 2015, *A&A*, 579, A19  
 Bailey S. I., 1902, *Ann. Harv. Coll. Obs.*, 38, 1  
 Blažko S., 1907, *Astron. Nachr.*, 175, 325  
 Bowman D. M., Kurtz D. W., 2014, *MNRAS*, 444, 1909  
 Buchler J. R., Moskalik P., 1992, *ApJ*, 391, 736  
 Chadid M., 2012, *A&A*, 540, A68  
 Gruberbauer M. et al., 2007, *MNRAS*, 379, 1498  
 Handberg R., Lund M. N., 2014, *MNRAS*, 445, 2698  
 Hertzsprung E., 1913, *Astron. Nachr.*, 196, 201  
 Howell S. B. et al., 2014, *PASP*, 126, 398  
 Jerzykiewicz M., Wenzel W., 1977, *Acta Astron.*, 27, 35  
 Jurešik J. et al., 2015, *ApJS*, 219, 25  
 Kolláth Z., Molnár L., Szabó R., 2011, *MNRAS*, 414, 1111  
 Kurtz D. W., 1985, *MNRAS*, 213, 773  
 Kurtz D. W., Shibahashi H., Murphy S. J., Bedding T. R., Bowman D. M., 2015, *MNRAS*, 450, 3015  
 Leavitt H. S., Pickering E. C., 1912, *Harv. Coll. Obs. Circ.*, 173, 1  
 Lenz P., Breger M., 2004, in Zverko J., Ziznovsky J., Adelman S. J., Weiss W. W., eds, *Proc. IAU Symp. 224, The A-Star Puzzle*. Cambridge Univ. Press, Cambridge, p. 786  
 Lund M. N., Handberg R., Davies G. R., Chaplin W. J., Jones C. D., 2015, *ApJ*, 806, 30  
 Molnár L. et al., 2015, *MNRAS*, 452, 4283  
 Montgomery M. H., O’Donoghue D., 1999, *Delta Scuti Star Newsl.*, 13, 28  
 Moskalik P., 2013, in Suárez J. C., Garrido R., Balona L. A., Christensen-Dalsgaard J., eds, *Proc. Astrophysics and Space Science, Vol. 31, Stellar Pulsations: Impact of New Instrumentation and New Insights*. Springer-Verlag, Berlin, p. 103  
 Moskalik P., 2014, in Guzik J. A., Chaplin W. J., Handler G., Pigulski A., eds, *Proc. IAU Symp. 301, Precision Asteroseismology*. Cambridge Univ. Press, Cambridge, p. 249  
 Moskalik P., Buchler J. R., 1990, *ApJ*, 355, 590  
 Moskalik P. et al., 2015, *MNRAS*, 447, 2348  
 Netzel H., Smolec R., Moskalik P., 2015a, *MNRAS*, 447, 1173  
 Netzel H., Smolec R., Moskalik P., 2015b, *MNRAS*, 453, 2022  
 Olech A., Moskalik P., 2009, *A&A*, 494, L17  
 Smolec R. et al., 2012, *MNRAS*, 419, 2407  
 Smolec R. et al., 2015a, *MNRAS*, 447, 3756  
 Smolec R. et al., 2015b, *MNRAS*, 447, 3873  
 Soszyński I. et al., 2011, *Acta Astron.*, 61, 1  
 Soszyński I. et al., 2014, *Acta Astron.*, 64, 177  
 Szabó R. et al., 2010, *MNRAS*, 409, 1244  
 Szabó R. et al., 2014, *A&A*, 570, A100  
 Tsessevich V. P., 1953, *Tr. Gos. Astron. Inst.*, 23, 62  
 Udalski A., Szymański M. K., Soszyński I., Poleski R., 2008, *Acta Astron.*, 58, 69  
 Udalski A., Szymański M. K., Szymański G., 2015, *Acta Astron.*, 65, 1  
 Vanderburg A., Johnson J. A., 2014, *PASP*, 126, 948  
 Wallerstein G., 2002, *PASP*, 114, 689

This paper has been typeset from a  $\text{\LaTeX}$  file prepared by the author.